Robotica (2017) volume 35, pp. 511–520. © Cambridge University Press 2015
doi:10.1017/S0263574715000661

A geometric approach for singularity analysis of 3-DOF planar parallel manipulators using Grassmann–Cayley algebra

Kefei Wen, TaeWon Seo* and Jeh Won Lee*

School of Mechanical Engineering, Yeungnam University, Gyeongsan 712–749, Republic of Korea

(Accepted July 16, 2015. First published online: August 17, 2015)

SUMMARY
Singular configurations of parallel manipulators (PMs) are special poses in which the manipulators cannot maintain their inherent infinite rigidity. These configurations are very important because they prevent the manipulator from being controlled properly, or the manipulator could be damaged. A geometric approach is introduced to identify singular conditions of planar parallel manipulators (PPMs) in this paper. The approach is based on screw theory, Grassmann–Cayley Algebra (GCA), and the static Jacobian matrix. The static Jacobian can be obtained more easily than the kinematic ones in PPMs. The Jacobian is expressed and analyzed by the join and meet operations of GCA. The singular configurations can be divided into three classes. This approach is applied to ten types of common PPMs consisting of three identical legs with one actuated joint and two passive joints.

KEYWORDS: Singularity; Planar parallel manipulators; Grassmann–Cayley Algebra; Screw theory; Plücker coordinates.

1. Introduction

Singular configurations of PPMs are special poses in which the manipulators cannot maintain their inherent infinite rigidity, meaning that subsequent behavior may be inscrutable. This leads to gaining uncontrollable degrees of freedom (DOFs).[1,2] Mathematically, the physical parameters (motions, forces, etc.) cannot be determined by the mathematical models such as kinematics equations or statics equations. Singular configurations should be avoided for a manipulator to be operated successfully. One way to avoid singularities is by path planning.[3] Another way to avoid singularities is eliminating the singular configurations. Several approaches have been suggested to eliminate the singularities of PPMs in the workspace, such as over-constraint[4,5] and actuator redundancy.[6,7] In both of these methods, the first step is to find the singularity configurations in the workspace.

The most common way to define a singular configuration is by defining the Jacobian matrices by differentiating the constraint equations of PPMs.[8] The method obtains the differential velocity equation $A\dot{x} + B\dot{q} = 0$ by differentiating the constraint equation, where $\dot{x}$ and $\dot{q}$ are the velocities of the end-effector and actuated joints, while A and B are Jacobian matrices. Three types of singular configurations are classified in this paper. Type-I singularities (inverse kinematics singularities) occur when $\det(B) = 0$. Type-II singularities (direct kinematics singularities) occur when $\det(A) = 0$. Type-III singularities occur when both $\det(A)$ and $\det(B)$ equal 0. Physically, Type-I singularities occur when a leg reaches the boundaries of the workspace, Type-II occurs when the end-effector is locally movable if all actuated joints are locked. A serial of examples contain ten types 3-DOFs PPMs to illustrate the corresponding configurations of these kind singularities will be given in Section 4.

A different approach to define singular configurations involves using twists.[9] The twist equation is obtained based on the notion of reciprocal screws in screw theory.[10] The formula can be written in the form of $Z\xi = \Lambda\dot{\theta}$, where ξ and $\dot{\theta}$ are the velocities of the end-effector and actuated joints, which have

* Corresponding author. E-mail: taewon_seo@yu.ac.kr, jwlee@yu.ac.kr

https://doi.org/10.1017/S0263574715000661 Published online by Cambridge University Press

Table I. Singularity analysis methods based on GCA.

Research	Characteristics
Ben-Horin *et al.*[16,17]	Singularity analysis on 6-DOF PM (Gough-Stewert platforms, and three leged robots)
Staffetti[18]	Instantaneous kinematic analysis on spatial PMs
Amine *et al.*[19]	Singularity analysis on 3T2R spatial PMs
Kanaan *et al.*[20]	Singularity analysis on lower mobility spatial PMs with no spherical joint
Proposed method	Singularity analysis on all types of 3-DOF planar parallel manipulators

a similar form to the $A\dot{x} + B\dot{q} = 0$. The singularity is classified in a similar way to that presented by Gosselin and Angeles.[8] The screw-based method has advantages of geometrical intuition and easy calculation without parameter differentiation.

Several studies have been conducted based on geometrical approaches to define the singular configurations.[11,12] The line geometry and linear complex approximation method were used to identify the singularity of a 3-DOF CaPaMan PM.[11] Degani and Wolf studied Maxwell's reciprocal figure theory method.[12] The method is convenient for describing one case of Type-II singularity in which three reciprocal screws of a PPM are intersecting at one point. However, the case of three reciprocal screws in parallel and Type-I singularities were not included.

Screw-based geometrical methods have advantages of geometrical intuition, so the method can be useful for the mechanism synthesis of rigid or flexure mechanisms. Huang *et al.* applied reciprocal screw theory to the type synthesis of symmetrical lower-mobility PMs, and they invented several novel manipulators based on this theory.[13] Kong *et al.*[14] used screw theory to synthesize 3-DOF spherical PMs. Yu *et al.*[15] explored a screw theory methodology for deterministic type synthesis of flexure mechanisms.

This paper focuses on investigating Type-I and Type-II singularities using the statics (or wrench) Jacobian matrix. For PPMs, the total wrench which acts on the moving platform is simply a linear combination of the corresponding force screws. This wrench Jacobian contains two 3×3 matrices, the same as in the twist equation. Every column vector in these two matrices can be transformed into a geometric entity using the reciprocal product operation of two screws and GCA. The singular conditions are found intuitively by observing the geometrical relationship of these geometric entities.

The contributions of this paper are as follows. First, the wrench Jacobian is derived by the join operation of GCA. The wrench Jacobian can be set up by a simple linear combination of three reciprocal screws defined by the join operation. Second, the method is a coordinate-free method, and the singular configurations can be found by intuitive observation without numerical calculation. Third, we classify two types of singular configurations via the physical meaning of the reciprocal actuating direction and the distance or angle of the actuator screws and reciprocal screws. Physically, the reciprocal actuating direction corresponds to the Type-II singularity, and the distance and angle metric gives the Type-I singularity. Moreover, the GCA-based method can be applied to all types of 3-DOF PPMs.

This research is not the first try to apply GCA to find a singularity of mechanisms. Table I summarized relevant papers of singularity analysis based on GCA. As you see in Table I, all the previous studies were tried to find the singularity of a full or lower DOF spatial PMs while this research aims to define the singularities of all types of 3-DOF PPMs. Because this paper analyzed singularities of all kinds of PPM, this research can be a good reference for researchers of mechanism theory. Also, from the geometric intuition of the proposed method, this method is very helpful to understand the motion of PPMs including singularities.

The rest of the paper is organized as follows. Wrenches and reciprocal screws are defined based on screw theory in Section 2, along with the join and meet operations of GCA. Section 3 presents the wrench statics based on the theoretical background of screw theory and GCA. The wrench Jacobian is defined by the linear combination of three reciprocal screws, and the results give a matrix composed of the reciprocal screws and distances/angles. In Section 4, the singular configurations of ten PPMs with different types of identical legs are analyzed geometrically. Concluding remarks are given in Section 5.

https://doi.org/10.1017/S0263574715000661 Published online by Cambridge University Press

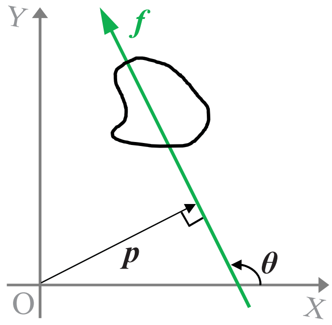

Fig. 1. Representation of a wrench on XY plane.

2. Theoretical Background

2.1. Wrenches and reciprocal screws

2.1.1. Representation of wrenches. In 3-dimensional Euclidean space, a force acting on a rigid body is expressed as a line in Plücker coordinates:

$$\hat{S} = (S; S^0)^T = (L, M, N; P, Q, R), \tag{1}$$

where L, M, and N are the magnitudes of the force, and P, Q, and R are the moments of the force with respect to the X, Y, and Z axes of the base coordinate frame, respectively. This is called a zero-pitch wrench (or zero-pitch force screw).[21] In a 2-dimensional plane, a wrench is reduced to (L, M; R)^T, and it can be separated into the magnitude of the force multiplied by a unit line segment along the screw axis:

$$\boldsymbol{w} = f\$ = f\,(c, s; p)^{\mathrm{T}}, \tag{2}$$

where $c = \cos\theta$ and $s = \sin\theta$, which denote the orientation of the line, and p is the perpendicular distance from the origin to the line, as shown in Fig. 1. $\$ = (c, s; p)^{\mathrm{T}}$ is also called a unit screw.

2.1.2. Distance between two screws. The reciprocal product of two zero pitch screws in space is given as:

$$\hat{S}_1 \circ \hat{S}_2 = S_1^T \cdot S_2^0 + S_2^T \cdot S_1^0 = -d \sin\varphi, \tag{3}$$

where $\circ$ denotes the reciprocal product operator, and $d = \|\mathbf{d}\|$ is the norm of $\mathbf{d}$, which is the common vertical line vector between $\hat{S}_1$ and $\hat{S}_2$. φ is the twist angle from $\hat{S}_1$ to $\hat{S}_2$, as illustrated in Fig. 2.

The distance between these two screws can be obtained by dividing by –sin φ on both sides of Eq. (3):

$$d = (\hat{S}_1 \circ \hat{S}_2)/(-\sin\varphi). \tag{4}$$

2.2. Grassmann–Cayley algebra

In this section, join and meet operations in GCA are introduced. GCA provides a symbolic approach for Plücker coordinates based on Grassmann's expansion.[22] It gives a convenient way to represent twists and wrenches.[23] In this section, some examples are used to introduce the main notions of join ($\vee$) and meet ($\wedge$) operations in 2-space.[24] More details on GCA can be found elsewhere.[25]

2.2.1. Join operation in 2-space. The join operation is used to define a line screw passing through two points. The configuration is shown in Fig. 3(a). A line on the XY plane expressed in the Plücker coordinate form may be obtained by the join of two distinct points, as shown in Fig. 3(a). The formula is as follows:

$$\mathbf{L} = \mathbf{a} \vee \mathbf{b} = \mathbf{ab} = \left(b_x - a_x, b_y - a_y; b_y a_x - a_y b_x\right)^{\mathrm{T}}, \tag{5}$$

in which the points $\mathbf{a}$ and $\mathbf{b}$ are expressed as the homogeneous coordinates $\mathbf{a} = (a_x a_y\ 1)$ and $\mathbf{b} = (b_x b_y\ 1)$, respectively.

https://doi.org/10.1017/S0263574715000661 Published online by Cambridge University Press

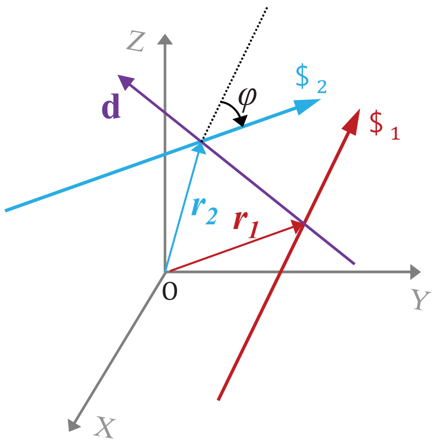

Fig. 2. Reciprocal product of two screws.

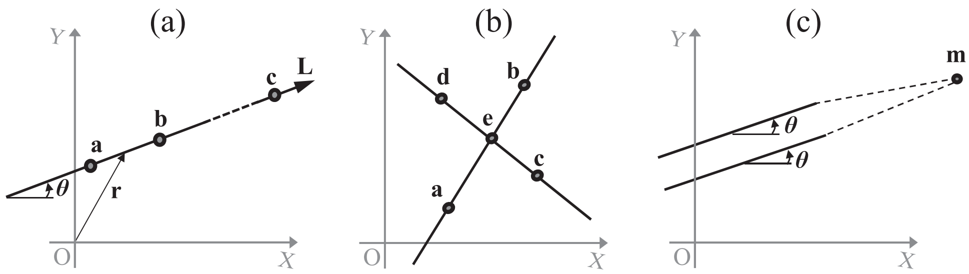

Fig. 3. Join and meet operations in GCA. (a) A line joined by two points. (b) Two lines meet at a point. (c) Two parallel lines meet at infinity.

If the point is assumed to be located at infinity, the point is assumed as $\mathbf{c} = (\cos\theta, \sin\theta, 0)$ in GCA, where the θ is the angle of the line as shown in Fig. 3(a). Note that $\mathbf{a}\vee\mathbf{c}$ and $\mathbf{b}\vee\mathbf{c}$ result in the same line, as shown in Fig. 3(a).

2.2.2. Meet operation in 2-space. The meet operation ($\wedge$) is used to determine the point of intersection between two lines. The point of intersection may be expressed as the meet of two lines. The configuration is shown in Fig. 3(b), and the equation is written as follows:

$$\mathbf{ab} \wedge \mathbf{cd} = [\mathbf{abc}]\mathbf{d} - [\mathbf{abd}]\mathbf{c} = \alpha\mathbf{e}, \tag{6}$$

where the brackets denote the determinant of the matrices, which contain the points as their columns, and α is a non-zero scalar that depends on the selection of points **a**, **b**, **c**, and **d**. A bracket will be zero when the same point appears more than once in the same bracket. Two parallel lines intersect at infinity, as shown in Fig. 3(c). If two lines are parallel, there is no intersection. However, in GCA, the intersection is at infinity, and the coordinates are assumed to be $\mathbf{m} = \alpha(\cos\theta, \sin\theta, 0)$, where θ is the angle of the parallel lines (Fig. 3(c)). Essentially, the intersection point **m** is the same as the infinite point **c** in Section 3.1. Using this characteristic, it is easy to calculate the intersection when two lines are parallel, because only the angle is required to determine the point. This characteristic is used to define the singularity configuration when the legs are parallel.

3. Statics of PPMs

3.1. Wrench equation by GCA

A wrench represented by Eq. (2) has a corresponding GCA representation involving the join of two distinct points on the screw axis, like in Eq. (5). Normalizing the last item in Eq. (5) yields

$$\mathbf{L} = f\,(c, s; p)^{\mathrm{T}} = f\overline{\mathbf{ab}}. \tag{7}$$

https://doi.org/10.1017/S0263574715000661 Published online by Cambridge University Press

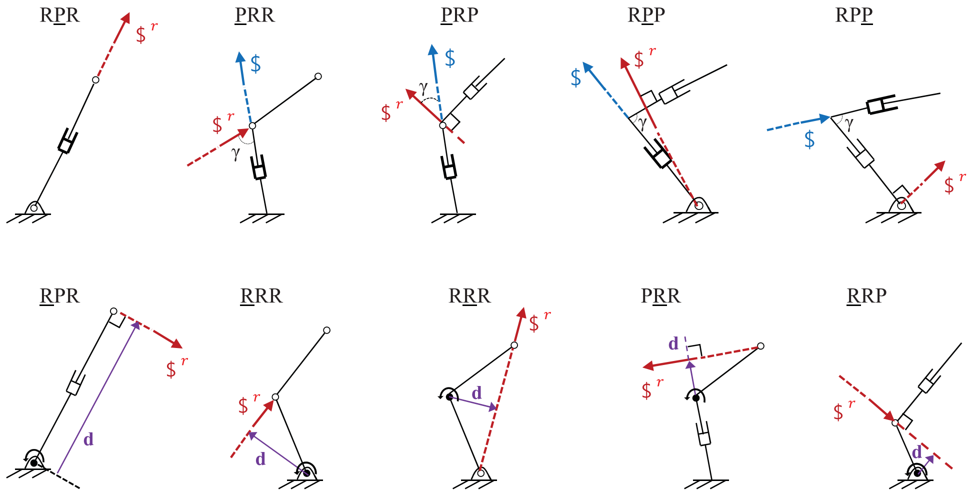

Fig. 4. Reciprocal wrenches of ten different types of legs. The underlines denote the actuated joints.

The distance between points **a** and **b** on the unit screw axis can be adjusted to achieve the appropriate magnitude of f.

3.2. *Reciprocal wrenches of PPMs*

Our main concern is 3-DOF PPMs, which are composed of three identical legs with only prismatic and revolute joints. Each leg consists of one actuated and two passive joints. These legs have ten different types of architectures. The probable reciprocal wrenches are illustrated in Fig. 4.

3.3. *Corresponding forces of actuated forces/torques*

The corresponding forces denote the forces whose active lines are on the reciprocal wrenches.[26] They are expressed as two types, depending on the prismatic or revolute actuated joints. For prismatic actuated joints, if the force along the joint screw axis is f, then the force f^r along the reciprocal wrench axis $\$^r$ can be expressed as

$$f^r = f \cdot \cos \angle f f^r. \tag{8}$$

The angle between f and f^r could be 0, γ, or $\pi/2 - \gamma$ for ($\mathrm{R\underline{P}R}$), ($\mathrm{\underline{P}RR}$, $\mathrm{\underline{P}RP}$), and ($\mathrm{R\underline{P}P}$, $\mathrm{RP\underline{P}}$) types of legs, respectively (Fig. 4). The values of the angles are constant except for the ($\mathrm{\underline{P}RR}$, $\mathrm{\underline{P}RP}$) type. For revolute actuated joints, if the torque along the revolute actuated joint screw axis is τ, then the force along the reciprocal wrench axis f^r can be expressed as

$$f^r = \tau / d, \tag{9}$$

where d is the vertical distance of the reciprocal screw and actuated joint screw, which was solved with Eq. (4).

3.4. *Statics equation of PPMs*

The statics equation is the linear combination of the reciprocal wrenches of each PPM.

$$\boldsymbol{w} = f_1^r \$_1^r + f_2^r \$_2^r + f_3^r \$_3^r. \tag{10}$$

For prismatic actuated PPMs, substituting Eqs. (8) and (9) into Eq. (10) yields

$$\boldsymbol{w} = \begin{bmatrix} \$_1^r & \$_2^r & \$_3^r \end{bmatrix} \boldsymbol{C} \begin{bmatrix} f_1 \\ f_2 \\ f_3 \end{bmatrix}, \text{ where } \mathbf{C} = \begin{bmatrix} c_1 & 0 & 0 \\ 0 & c_2 & 0 \\ 0 & 0 & c_3 \end{bmatrix} \tag{11}$$

https://doi.org/10.1017/S0263574715000661 Published online by Cambridge University Press

in which $c_i = \cos\angle f_i f_i^r$, $i = 1, 2, 3$. The following is obtained for revolute actuated PPMs:

$$\boldsymbol{w} = \begin{bmatrix} \$_1^{\mathrm{r}} & \$_2^{\mathrm{r}} & \$_3^{\mathrm{r}} \end{bmatrix} \mathbf{D} \begin{bmatrix} f_1 \\ f_2 \\ f_3 \end{bmatrix}, \text{ where } \mathbf{D} = \begin{bmatrix} 1/d_1 & 0 & 0 \\ 0 & 1/d_2 & 0 \\ 0 & 0 & 1/d_3 \end{bmatrix}. \quad (12)$$

Equations (11) and (12) are abbreviated with the following form:

$$\boldsymbol{w} = \mathbf{J}\boldsymbol{\lambda}, \quad (13)$$

where $\mathbf{J} = \mathbf{J}_1\mathbf{J}_2$ is the wrench Jacobian, here $\mathbf{J}_1 = [\$_1^{\mathrm{r}} \quad \$_2^{\mathrm{r}} \quad \$_3^{\mathrm{r}}]$, $\mathbf{J}_2 = \mathbf{C}$, while $\boldsymbol{\lambda} = [f_1\, f_2\, f_3]^{\mathrm{T}}$ for prismatic actuated PPMs and $\mathbf{J_2} = \mathbf{D}$, while $\boldsymbol{\lambda} = [\tau_1\tau_2\tau_3]^{\mathrm{T}}$ for revolute actuated PPMs.

If $\det(\mathbf{J}_2) = 0$, one or more legs in a PPM will reach the boundaries of the workspace, this is similar to the case of $\det(\mathbf{B}) = 0$ in Section 1. Therefore, $\det(\mathbf{J}_2) = 0$ corresponds to Type-I singularity. While $\det(\mathbf{J}_1) = 0$ is similar to $\det(\mathbf{A}) = 0$. It is not obvious but we will see in the next Section, $\det(\mathbf{J}_1) = 0$ occurs when the three legs of a PPM are intersect at one point or parallel to each other, this provides a locally DOF for the PPM, then $\det(\mathbf{J}_1) = 0$ corresponds to the Type-II singularity. As mentioned in Section 2, the columns in $\mathbf{J}_1$ are actually the normalized Plücker coordinates of the join of two distinct points on the screw axis. Then, the determinant of $\mathbf{J}_1$ may be transformed into the bracket algebra form[27] as follows:

$$\det(j_i) = \left[\overline{\mathrm{A}_1\mathrm{B}_1}, \overline{\mathrm{A}_2\mathrm{B}_2}, \overline{\mathrm{A}_3\mathrm{B}_3}\right], \quad (14)$$

where $\overline{\mathrm{A}_1\mathrm{B}_1}$, $\overline{\mathrm{A}_2\mathrm{B}_2}$, and $\overline{\mathrm{A}_3\mathrm{B}_3}$ denote the normalized lines of $\mathrm{A}_1\mathrm{B}_1$, $\mathrm{A}_2\mathrm{B}_2$, and $\mathrm{A}_3\mathrm{B}_3$, respectively. And A_i, B_i (i = 1,2,3) are two different points on $\$_i^r$.

The situation where $\det(\mathbf{J}_1) = 0$ is identical to

$$[\mathrm{A}_1\mathrm{B}_1, \mathrm{A}_2\mathrm{B}_2, \mathrm{A}_3\mathrm{B}_3] = 0. \quad (15)$$

$[\mathrm{A}_1\mathrm{B}_1, \mathrm{A}_2\mathrm{B}_2, \mathrm{A}_3\mathrm{B}_3]$ can be translated into a Grassmann–Cayley expression by implementing Cayley factorization:[28]

$$[\mathrm{A}_1\mathrm{B}_1, \mathrm{A}_2\mathrm{B}_2, \mathrm{A}_3\mathrm{B}_3] = [\mathrm{A}_1\mathrm{B}_1\mathrm{A}_3]\,[\mathrm{A}_2\mathrm{B}_2\mathrm{B}_3] - [\mathrm{A}_1\mathrm{B}_1\mathrm{B}_3]\,[\mathrm{A}_2\mathrm{B}_2\mathrm{A}_3] = \mathrm{A}_1\mathrm{B}_1 \wedge \mathrm{A}_2\mathrm{B}_2 \wedge \mathrm{A}_3\mathrm{B}_3, \quad (16)$$

which is the meet of the three lines. As said in Section 2.2.b, any bracket in the middle part of Eq. (16) will be zero if a same point appears more than once in the same bracket. For example, if A_2 and B_2 are located in a same position, the second and fourth brackets equal 0 and then Eq. (16) will be 0–0 = 0. This provides a convenient geometric method for singularity analysis.

4. Singularity Analysis of PPMs

4.1. Singularity analysis of 3-R<u>P</u>R PPMs

For this type of PPMs, the angle between $f f^r$ is 0. Therefore, a Type-I singularity does not exist, while Type-II singularities occur in two cases. In case 1, three lines intersect at one point m, while in case 2, the three lines are parallel to each other, which is also understood as the intersection point m being at infinity, as in Eq. (17). The two possible singularity configurations in these situations are illustrated in Fig. 5. The equations of the singularities can be expressed with the same form:

$$[\mathrm{A}_1\mathrm{M},\ \mathrm{A}_2\mathrm{M},\ \mathrm{A}_3\mathrm{M}] = [\mathrm{A}_1\mathrm{M}\mathrm{A}_3]\,[\mathrm{A}_2\mathrm{M}\not{\mathrm{M}}] - [\mathrm{A}_1\mathrm{M}\not{\mathrm{M}}]\,[\mathrm{A}_2\mathrm{M}\mathrm{A}_3] = 0. \quad (17)$$

4.2. Singularity analysis of 3-<u>P</u>RR and 3-<u>P</u>RP PPMs

The corresponding forces of these types of PPMs pass through two revolute joints and form an angle γ_i with the prismatic joint on each leg. It is convenient to select six points located in the R joints, as

https://doi.org/10.1017/S0263574715000661 Published online by Cambridge University Press

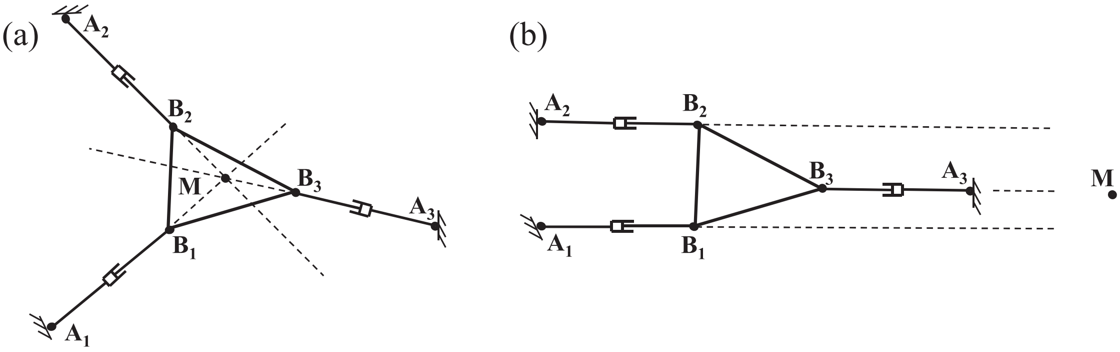

Fig. 5. The Type-II singular configurations of a 3-RPR PPM. (a) Three legs are concurrent. (b) Three legs are parallel.

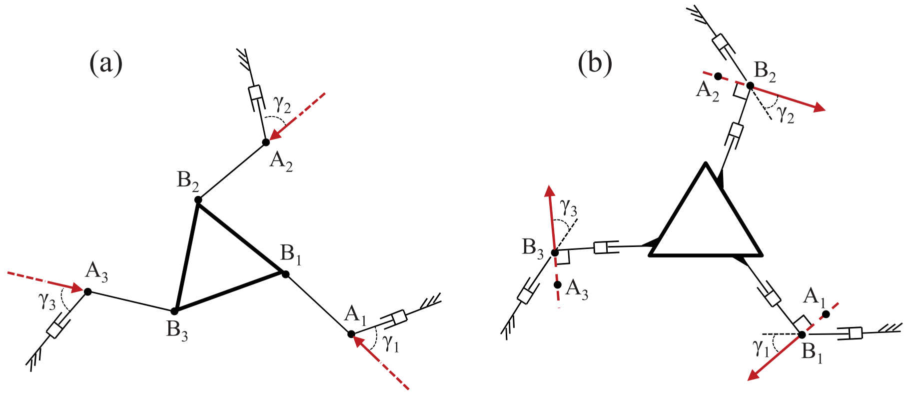

Fig. 6. 3-DOF PPMs with P actuated legs of (a) A 3-PRR PPM. (b) A 3-PRP PPM.

shown in Fig. 6(a). The Jacobian j_2 of 3-PRR PPMs is

$$j_2 = \begin{bmatrix} \cos\gamma_1 & 0 & 0 \\ 0 & \cos\gamma_2 & 0 \\ 0 & 0 & \cos\gamma_3 \end{bmatrix}. \tag{18}$$

Type-I singularities occur when $\cos\gamma_i = \pi/2$ for at least one value of i. In these configurations, the RR link is perpendicular to the P joint in each leg. Referring to Eq. (16), in order to obtain j_1, it is convenient to select six points located in the R joints, as shown in Fig. 6(a). The Type-II singularities occur when all three lines A_iB_i are concurrent or parallel to each other.

The corresponding forces of 3-PRP PPMs are always through the R joint and intersect at right angles with the distal link. It is possible to select two points to confirm the orientation of each corresponding force, with one at the R joint and another one outside the leg but located on the reciprocal wrench axis. The Jacobians of these types of PPMs have the same form as 3-PRR PPMs. Type-I singularities occur when the two P joints in a leg are parallel.

For Type-II singularity analysis, the orientations of the corresponding forces are not independent of the distal legs, as shown in Fig. 6(b). The positional relations of the three distal legs are constant during all working modes. For an appropriate design, these legs will not be concurrent or parallel to each other.

4.3. Singularity analysis of 3-RPP and 3-RPP PPMs

In Fig. 7(a), the corresponding forces are through R joints and normal to the distal link in each leg, while they are normal to the first link in Fig. 7(b). The Jacobian B is always constant for both types of PPMs, so there are no Type-I singularities. The reciprocal wrenches of 3-RPP PPMs have the same geometrical configuration as those of 3-PRP PPMs, so they have similar results regarding

https://doi.org/10.1017/S0263574715000661 Published online by Cambridge University Press

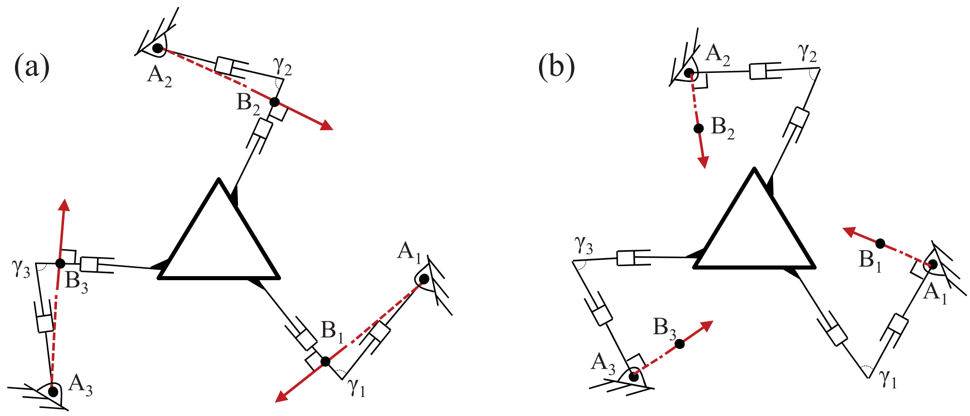

Fig. 7. 3-DOF PPMs with P actuated legs of (a) A 3-RPP PPM. (b) A 3-RPP PPM.

Type-II singularities. This type of singularity for 3-RPP PPMs will also occur when the three lines are concurrent.

4.4. Singularity analysis of PPMs with revolute actuated joint

This section investigates the five remaining types of PPMs (3-RPR, 3-RRR, 3-RRR, 3-PRR, and 3-RRP), which use revolute actuated joints. In contrast to previous configurations, these PPMs translate the actuated torques into corresponding forces. The singularity configurations may be found more intuitively by using GCA. In these cases, the Jacobian j_2 is expressed as

$$j_2 = \begin{bmatrix} 1/d_1 & 0 & 0 \\ 0 & 1/d_2 & 0 \\ 0 & 0 & 1/d_3 \end{bmatrix}. \tag{19}$$

For 3-RPR PPMs, the corresponding forces pass through the passive R joints and are normal to P joints. The Type-I singularities occur when two R joints in any one leg coincide with each other, because the distance d in this leg is 0, as shown in Fig. 8(a). Type-II singularity conditions are the same as for 3-RPR PPMs, occurring when the three lines are concurrent. The possible singularity configurations of both types are illustrated in Fig. 8(b).

The 3-RRR and 3-RRR PPMs have the same static characteristics. The corresponding forces are along the lines which pass through the two passive joints in each leg. There are two different architectures when the PPMs are in Type-I singularities, in which the three R joints are collinear, or the first and finial R joints coincide in a leg. The Type-II singularities can be found simply when the three lines are concurrent. Two different possible Type-I singularity configurations of both types of PPMs are shown in Fig. 9.

The 3-PRR and 3-RRP PPMs can be considered together since the corresponding forces of each leg are always passing through the passive R joints and normal to the P joints. This is the same as 3-RPR PPMs. The singularity analysis procedure is the same, but the Type-I singularities occur when the first and distal links are perpendicular in a leg.

4.5. Summary of singularity analysis for PPMs

All of the ten types of PPMs can be divided into four groups according to the determinants of j_1 and j_2. The 3-RPR, 3-RPP, and 3-RPP PPMs have Type-II singularities only, while the 3-PRP PPMs have only Type-I singularities. The 3-PRR and the five types of R actuated PPMs both have Type-I and Type-II singularities, but the condition determining Type-II singularities is different. Table II gives the result of singularity analysis for the ten types of PPMs.

4.6. Singularity analysis of non-identical legs PPMs

The GCA based method is also available to the singularity analysis of those 3-DOF PPMs with non-identical legs. The analysis procedure is the same as identical legs PPMs. For any type legs,

https://doi.org/10.1017/S0263574715000661 Published online by Cambridge University Press

Table II. The result of singularity analysis for the ten types of PPMs.

Type of PPM	$\text{Det}(j_1) = 0$	$\text{Det}(j_2) = 0$
3-R$\underline{\text{P}}$R, 3-R$\underline{\text{P}}$P, 3-RP$\underline{\text{P}}$	$* \equiv$	Not existed
3-$\underline{\text{P}}$RR	$* \equiv$	Any $\cos\gamma_i = 0$
3-$\underline{\text{P}}$RP	Not existed	Any $\cos\gamma_i = 0$
Five types of $\underline{\text{R}}$ actuated PPMs	$* \equiv$	Any $d_i = 0$

*: Three lines intersect at one point. $\equiv$: Three lines are parallel.

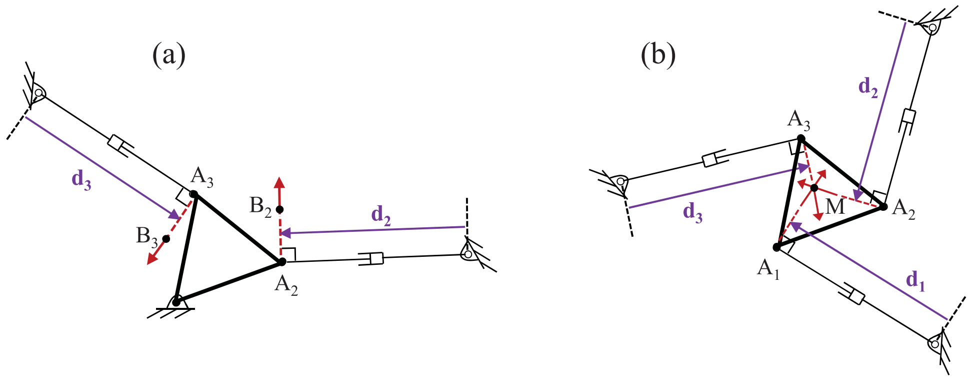

Fig. 8. Possible singularity configurations of a 3-R$\underline{\text{P}}$R PPM. (a) Type-I singularity. (b) Type-II singularity.

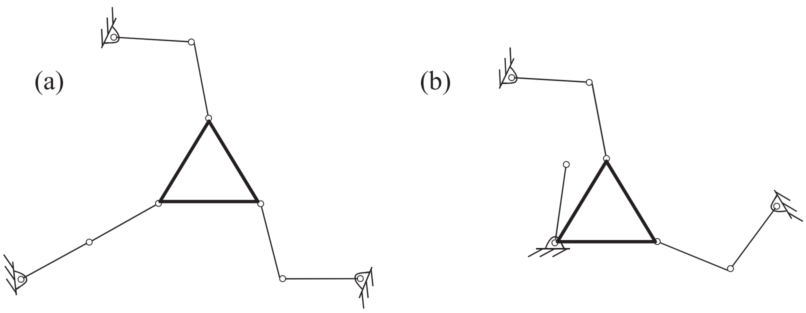

Fig. 9. Two different configurations of Type-1 singularity for 3-$\underline{\text{R}}$RR and 3-R$\underline{\text{R}}$R PPMs. (a) A leg is fully extended. (b) A leg is folded.

using Eqs. (8) and (9), we can obtain the force f^r along the reciprocal wrench axis $\$^r$. Subsequently, find $\mathbf{J}_1$ and $\mathbf{J}_2$ from Eq. (11) or (12). The rest is to inspect $\det(\mathbf{J}_1)$ and $\det(\mathbf{J}_2)$.

5. Conclusion

The singularity configurations of ten types of PPMs have been analyzed geometrically using GCA. The GCA is a coordinate-free method and does not require calculation of the inverse Jacobian matrix. The results show that all of the R actuated PPMs have both Type-I and Type-II singularities, but this is not exactly true for the P actuated PPMs. For example, the 3-R$\underline{\text{P}}$R, 3-R$\underline{\text{P}}$P, and 3-RP$\underline{\text{P}}$ PPMs have only Type-II singularities, while the 3-$\underline{\text{P}}$RP PPMs have only Type-I singularity. This means that the motion of these PPMs has just one type of singularity and will be more dexterous, so they will be easier to control.

There is limitation of the research that since this method found sufficient condition for the singularity, the method cannot guarantee all the singularities are found. Therefore, further discussion is necessary to find the necessary condition of all the singularities.

https://doi.org/10.1017/S0263574715000661 Published online by Cambridge University Press

Acknowledgements
This study was supported by the Basic Science Research Program through the National Research Foundation of Korea (NRF), funded by the Ministry of Education (NRF-2014R1A1A4A01009290).

References

1. K. H. Hunt, "Structural kinematics of in-parallel actuated robot arms," *J. Mech. Transm.-T. ASME*, **105**(4), 705–712 (1983).
2. J. P. Merlet, *Parallel Robot* (Dordrecht, The Netherlands, Springer, 2nd ed. 2006).
3. A. K. Dash, I. Chen, S. H. Yeo and G. Yang, "Singularity-Free path Planning of Parallel Manipulators using Clustering Algorithm and Line Geometry," *Proceedings of the 2003 IEEE International Conference on Robotics and Automation*, Taipei, Taiwan (Sept. 14–19, 2003).
4. Y. H. Chung, J. H. Choo and J. W. Lee, "SenSation: A New 2-DOF Parallel Mechanism for Haptic Device," *Proceedings 2nd Workshop on Computational Kinematics*, Seoul, South Korea (May 20–22, 2001) pp. 45–56.
5. G. F. Liu, Y. L. Wu, X. Z. Wu, Y. Y. Kuen and Z. X. Li, "Analysis and Control of Redundant Parallel Manipulators," *Proceedings of the 2001 IEEE International Conference on Robotics and Automation*, Seoul, Korea (May 21–26, 2001).
6. J. A. Saglia, J. S. Dai and D. G. Caldwell, "Geometry and kinematic analysis of a redundantly actuated parallel mechanism that eliminates singularities and improves dexterity," *J. Mech. Des.* **130**(12), 124501 (2008).
7. I. Ebrahimi, J. A. Carretero and R. Boudreau,"3-PRRR redundant planar parallel manipulator: Inverse displacement, workspace, and singularity analysis," *Mech. Mach. Theory* **42**(8), 1007–1016 (2007).
8. C. Gosselin and J. Angeles, "Singularity analysis of closed-loop kinematic chains," *IEEE Trans. Robot. Autom.* **6**(3), 281–290 (1990).
9. I. A. Bonev, D. Zlatanov and C. M. Gosselin, "Singularity analysis of 3-DOF planar parallel mechanisms via screw theory," *J. Mech. Des.* **125**, 573–581 (Sept. 2003).
10. J. K. Davidson and K. H. Hunt, *Robots and Screw Theory* (Oxford University Press, Oxford, 2004).
11. A. Wolf, E. Ottaviano, M. Shoham and M. Ceccarelli, "Application of line geometry and linear complex approximation to singularity analysis of the 3-DOF CaPaMan parallel manipulator," *Mech. Mach. Theory* **39**, 75–95 (2004).
12. A. Degani and A. Wolf, "Graphical Singularity Analysis of Planar Parallel Manipulators," *Proceedings of the 2006 IEEE International Conference on Robotics and Automation*, Orlando, Florida (May, 2006).
13. Z. Huang and Q. C. Li, "General methodology for type synthesis of symmetrical lower-mobility parallel manipulators and several novel manipulators," *Int. J. Robot. Res.* **21**(2), 131–145 (2002).
14. X. Kong and C. M. Gosselin, "Type synthesis of 3-DOF spherical parallel manipulators based on screw theory," *J. Mech. Des.* **126**(1), (2004).
15. J. Yu, S. Li, H. Su and M. L. Culpepper, "Screw theory based methodology for the determinisitic type synthesis of flexure mechanisms," *J. Mech. Robot.* **3**(3), 031008 (2011).
16. P. Ben-Horin and M. Shoham, "Singularity analysis of a class of parallel robots based on Grassmann–Cayley algebra," *Mech. Mach. Theory* **41**(8), 958–970 (2006).
17. P. Ben-Horin and M. Shoham, "Singularity condition of six-degree-of-freedom three-legged parallel robots based on Grassmann–Cayley algebra," *IEEE Trans. Robot.* **22**(4), 577–590 (2006).
18. E. Staffetti, "Kinestatic analysis of robot manipulators using the Grassmann–Cayley algebra," *IEEE Trans. Robot. Autom.* **20**(2), 200–210 (2004).
19. S. Amine, M. T. Masouleh, S. Caro, P. Wenger and C. Gosselin, "Singularity analysis of 3T2R parallel mechanisms using Grassmann–Cayley algebra and Grassmann geometry," *Mech. Mach. Theory* **52**, 326–340 (2012).
20. D. Kanaan, P. Wenger, S. Caro and D. Chablat, "Singularity analysis of lower-mobility parallel manipulators using Grassmann-Cayley Algebra," *IEEE Trans. Robot.* **25**(5), 995–1004 (2009).
21. Z. Huang, Y. S. Zhao and T. S. Zhao, *Advanced Spatial Mechanism* (Beijing, P. R. China, Higher Education Press, 2006), ch, 1.
22. N. L. White, "Grassmann–Cayley Algebra and Robotics Applications," **In**: *Handbook of Geometric Computing* (E. B. Corrochano, ed.) (Berlin Heidelberg, Springer-Verlag, 2005) pp. 629–656.
23. E. Staffetti, "Kinestatic analysis of robot manipulators using the Grassmann–Cayley algebra," *IEEE Trans. Robot. Autom.* **20**, 200–210 (Apr. 2004).
24. P. Doubilet, G.-C. Rota and J. Stein, "On the foundations of combinatorial theory: IX combinatorial methods in invariant theory," *Stud. Appl. Math.* **53**(3), 185–216 (1974).
25. P. Ben-Horin and M. Shoham, "Application of Grassmann–Cayley algebra to geometrical interpretation of parallel robot singularities," *Int. J. Robot. Res.* **28**(1), 127–141 (2009).
26. J. H. Choi, T. W. Seo and J. W. Lee, "Singularity analysis of a planar parallel mechanism with revolute joints based on a geometric approach," *Int. J. Precis. Eng. Manuf.* **14**(8), 1369–1375 (2013).
27. N. L. White, "The bracket of 2-extensors," *Congressus Numerantium*, **40**, 419–428 (1983).
28. N. L. White and T. McMillan, Cayley Factorization, *IMA Preprint Series* # 371, University of Minenesota, 206 Church St, S.E., Minneapolis, MN, USA (1987).

https://doi.org/10.1017/S0263574715000661 Published online by Cambridge University Press